Journal of Photochemistry & Photobiology, A: Chemistry 462 (2025) 116205

Contents lists available at ScienceDirect

Journal of Photochemistry & Photobiology, A: Chemistry

journal homepage: www.elsevier.com/locate/jphotochem

Combined experimental and modellistic approach to unravel the pH dependence of photocatalytic hydrogen production

Fabrizio Sordello *

Dipartimento di Chimica, Università degli Studi di Torino, Italy

ARTICLE INFO

Keywords:
Photocatalysis
Hydrogen production
Kinetic model
pH dependence
Photocatalytic reforming

ABSTRACT

Hydrogen production via formic acid reforming on Pt-loaded TiO_2 was characterized by marked pH dependence with higher rates at acidic pH, a maximum around pH 4, and a sharp decrease at pH 5–6. We observed a similar behavior with methanol reforming. With formic acid, hydrogen and CO_2 production rates were within the limits of experimental errors, while with methanol, CO_2 evolution was delayed because of the formation of partially oxidized C1 intermediates. We observed the same trends photodepositing Pt from hexachloroplatinic acid in a preceding irradiation experiment at fixed pH, thereby demonstrating that Pt photodeposition was not responsible for the observed pH-dependence. We modelled the photocatalytic process to account for pH dependence by analyzing the rate constant for the oxidation of formic acid promoted by valence band holes. Our study demonstrates that the electrostatic interaction between substrate and TiO_2 surface is the cause of the pH dependence of hydrogen production rate.

1. Introduction

The conversion of solar energy into electricity and high added value chemicals will gain importance in the next decades, [1,2] and the feasibility of photoelectrochemical cells for water splitting [3,4] has already been demonstrated. Even though many challenges remain, [5–8] H_2 production from solar light at high efficiency is possible. [9,10] Research is very active both in the improvement of photoelectrochemical cells [11] and in the field of organics reforming [12,13] and artificial photosynthesis. [14,15] These achievements are the result of the deeper understanding of the phenomena and reaction mechanisms involved, which is, in turn, the basis for future development.

With respect to photocatalytic H_2 production, many rigorous studies have been published, focusing on various aspects of the process, and especially on the photocatalyst development. [16–19] Limiting our analysis to TiO_2 in the presence of co-catalysts for H_2 evolution, particular attention has been devoted to the oxide structure, as well as exploring different nanoparticle shapes, to improve the charge carrier separation [20,21] and three dimensional morphology [22] to maximize the absorption of incoming light. Similar attention has been devoted to the co-catalyst for H_2 production [23–26] and to the sacrificial hole scavenger employed. [27–29] Methanol reforming on Pt-loaded TiO_2 produces mainly H_2, HCHO, CO_2 and HCOOH, with their ratio dependent on the noble metal co-catalyst and on the kind of TiO_2 employed, whereas CH_4 and CO are minor products. [30] Conversely, the reforming of superior alcohols produces significant amounts of CH_4 and/or higher hydrocarbons, depending on the molecular structure, in addition to H_2 and CO_2. [29].

While the effects of many variables have been studied in detail, pH dependence is seldom investigated, and usually only marginally if it is, compared with other aspects, [31] or with a qualitative and sometimes naive approach, even in recent years. [32–34] Therefore, the aim of the present work is to investigate and understand the effect of pH on photocatalytic formic acid and methanol reforming by means of a combined experimental and modellistic approach. Notwithstanding the difference between the two hole scavengers employed, particularly evidenced at low concentrations, a substantial similarity emerged, which we tried to unravel by firstly modelling the kinetics of the overall photocatalytic process and then analyzing the electrostatic component of the rate constant related to the reaction of formic acid with TiO_2 photoholes.

Abbreviations: SI, Supporting Information.

* Address: Via Pietro Giuria 7, 10125 Torino, Italy.
E-mail address: fabrizio.sordello@unito.it.

https://doi.org/10.1016/j.jphotochem.2024.116205
Received 4 October 2024; Received in revised form 15 November 2024; Accepted 1 December 2024
Available online 5 December 2024

2. Experimental

2.1. Chemicals

TiO_2 P25 was a gift from Degussa; hexachloroplatinic acid hexahydrate (37.5% Pt basis), formic acid (85% in water) and methanol (99.9%) were purchased from Aldrich; and sodium formate (99%) was purchased from Merck. All the reagents were used without further purification.

2.2. Hydrogen production

Hydrogen production experiments were performed by the irradiation with UV light of slurries containing 1.0 g L^{-1} of P25 TiO_2 powder and 2.0 mg L^{-1} of Pt, added as H_2PtCl_6, which is reduced to Pt(0) and deposited onto TiO_2 upon the very first minutes of irradiation. Formic acid or methanol was used as the hole scavenger at different concentrations. The addition of $HClO_4$ was used to control the pH of the suspensions in the range of 1.4–5; phosphate buffer 10 mM in the range of 6–8; bicarbonate/carbonate buffer 10 mM in the range of 10–11; and NaOH in the range of 12–14. Only in the case of HCOOH in the pH range of 2.8–4.8 was formic acid used as both hole scavenger and pH buffer. The irradiation experiments were carried out in magnetically stirred, cylindrical quartz cells (3.5 cm inner diameter, 2 cm height) containing 5 mL of slurry. Before irradiation the cell containing the slurry was carefully purged with nitrogen to remove oxygen from the reaction environment. To study the effect of Pt deposition we synthesized the material pH3-Pt-P25 by irradiating a slurry at pH 3 containing P25 TiO_2 1.0 g L^{-1}, Pt (as H_2PtCl_6) 2.0 mg L^{-1} and CH_3OH 0.10 M for 30 min. The slurry was then centrifuged, and the white-grayish powder obtained was washed with MilliQ water several times, dried in an oven at 60 °C overnight and stored for later use.

Hydrogen and CO_2 evolution were monitored by periodically withdrawing 2.5 mL of gas from the irradiation cell and replacing it with the same volume of N_2. The gas sample was analysed with an Agilent 4900 Micro GC gas chromatograph equipped with a Molsieve 5Å and a PoraPlot U column for H_2 and CO_2 analysis, respectively. During the analysis, the columns were kept at a temperature of 90 °C and 40 °C and at a pressure of 200 kPa and 150 kPa; the carrier gases were argon and helium, respectively. The total amount of H_2 produced as a function of time was calculated from the concentration in the sampled gas, from the volume of gas in the irradiation cell and considering previous samplings. Rates were obtained from the slope of the gas produced as a function of time. Rates were constant for the duration of the runs (at least 50–60 min) with $R^2 > 0.99$. The radiation source was a Philips PLS-10 lamp located at a distance of 10 cm from the quartz cell, with a flat sheet of Al foil as a reflector (Fig. S1 in SI). The lamp emission was centered at 365 nm and the irradiance at the top of the solutions was 78 W m^{-2}, measured with a CO.FO.ME.GRA. power meter.

3. Results

When formic acid was used as a hole scavenger, the hydrogen production rate exhibited a maximum of 6.3 10^{-2} mmol g^{-1} min^{-1} around pH 4, after which it rapidly decayed to 5.0 10^{-3} mmol g^{-1} min^{-1} at pH 6 and below 6.9 10^{-4} mmol g^{-1} min^{-1} at basic pH values (Fig. 1). Below pH 4, we observed a smoother decrease of the hydrogen production rate with decreasing pH. The CO_2 production rate showed the same behaviour. Moreover, below pH 5, the CO_2 and H_2 production rates coincide, because HCOOH is oxidized to CO_2 without the accumulation of intermediates and both H_2 and CO_2 evolution require the transfer of two electrons. On the other hand, above pH 6, the CO_2 production rate is one order of magnitude lower compared with H_2 because of the pH equilibria involving CO_2, HCO_3^- and CO_3^{2-}. Neither CH_4 nor CO was detected during the analysis. A trend similar to that exhibited by the H_2 production rate, with a maximum and a rapid rate decrease at neutral pH,

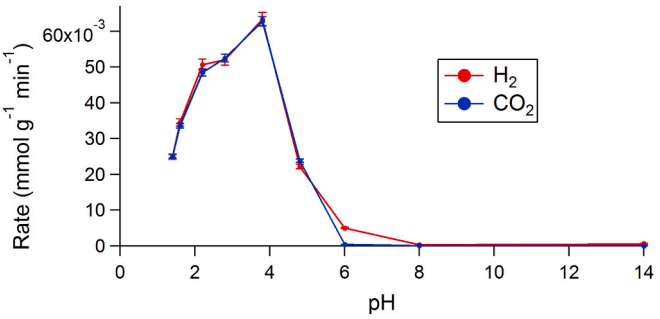

Fig. 1. H_2 and CO_2 production rates as functions of the pH for irradiated slurries containing 1 g L^{-1} of P25 TiO_2 and 2 mg L^{-1} of Pt in the presence of HCOOH 0.1 M.

was found for propionic acid [31] and also CH_3OH, even though, in this case, the H_2 production rate plateau at neutral and basic pH was at a higher value (1.0–1.5 10^{-2} mmol g^{-1} min^{-1} Fig. 2). Because CH_3OH oxidation to CO_2 requires six electrons, and therefore intermediate accumulation (HCHO, HCOOH) is possible in this case, CO_2 production rate is significantly slower compared with H_2, even at acidic pH, where the formation of HCO_3^- is negligible. With CH_3OH as an electron scavenger, traces of CH_4 and CO were detected for the highest irradiation times only, in agreement with previous reports. [29,30].

We highlighted the difference between the two electron scavengers studied in the present work using lower concentrations: 1 mM for HCOOH and 0.25 mM for CH_3OH. In the presence of HCOOH, CO_2 evolution matched H_2 production almost perfectly; however, in the case of CH_3OH, CO_2 formation was slower and delayed (Fig. 3). In particular, after 60 min, both H_2 and CO_2 production rates increased and were closer in magnitude compared with the first 40 min of irradiation, evidencing the formation of oxidised intermediates, [30] including HCOOH, which are more readily oxidized to CO_2 (Fig. 3b). In both cases, because of substrate depletion, equilibrium is reached in the final minutes of irradiation and indeed gas evolution stops.

The effect of pH on the H_2 and CO_2 production rates was similar, irrespective of the hole scavenger employed. With both HCOOH and CH_3OH we observed higher rates at acidic pH and a sharp decrease at neutral pH (Fig. 1 and Fig. 2). To understand if Pt deposition at different pH values could have caused the trends observed, [35] we synthesized a Pt-loaded P25 at pH 3 (pH3-Pt-P25) and used the material for the photocatalytic reforming of methanol at different pH values. Even if the rates are lower (Fig. 4) compared with the previous experiment (Fig. 2), we observed very similar trends for H_2 and CO_2 production rate, with higher rates at acidic pH values and lower activity at neutral and basic pH values (Fig. 4). This suggests that Pt deposition was not responsible for the pH dependence of the observed rates.

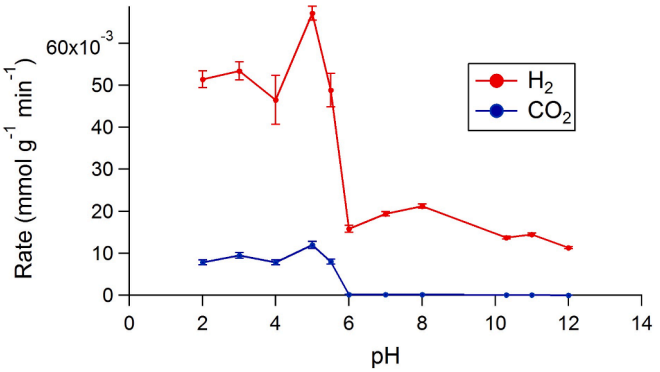

Fig. 2. H_2 and CO_2 production rates as functions of the pH for irradiated slurries containing 1 g L^{-1} of P25 TiO_2 and 2 mg L^{-1} of Pt in the presence of CH_3OH 0.1 M.

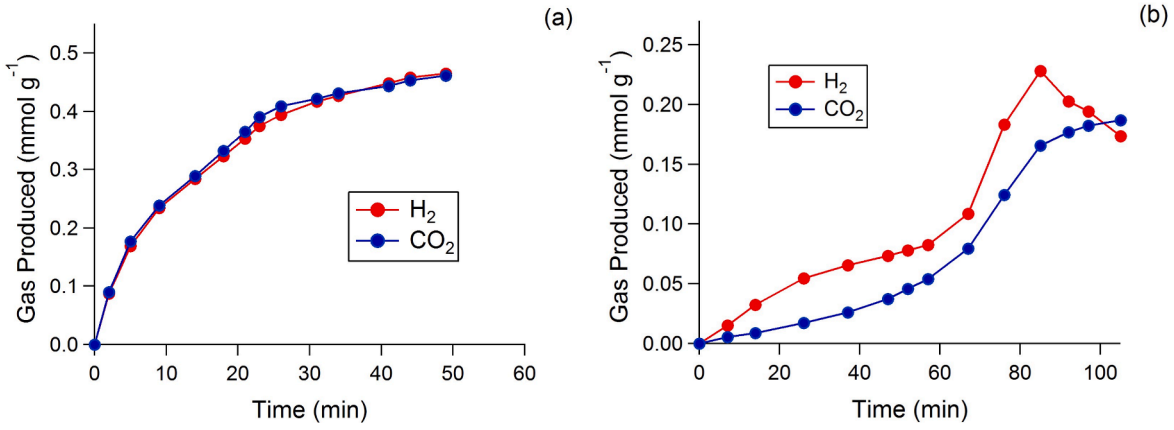

Fig. 3. H_2 and CO_2 evolved as functions of the irradiation time for irradiated slurries containing 1 g L^{-1} of P25 TiO_2 and 2 mg L^{-1} of Pt in the presence of HCOOH 1 mM (a) or CH_3OH 0.25 mM (b).

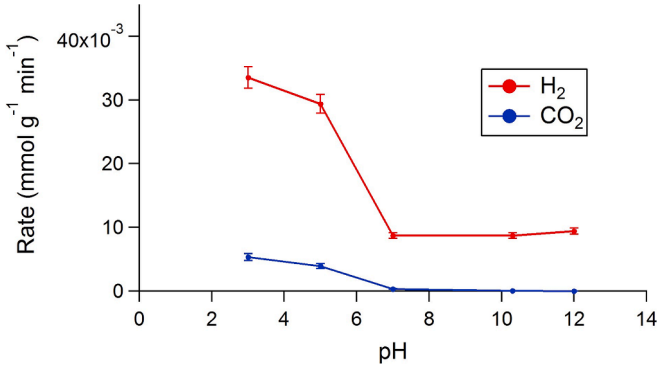

Fig. 4. H_2 and CO_2 production rates as functions of the pH for irradiated slurries containing 1 g L^{-1} of pH3-Pt-P25 TiO_2 in the presence of CH_3OH 0.1 M.

4. Discussion

To understand the causes behind these phenomena, we modelled the photocatalytic process by adapting the general case [36] to formic acid reforming, considering the formation of the photogenerated holes h^+ and electrons e^- (Eq. (1)):

$$h\nu \xrightarrow{\varphi} e^- + h^+ \tag{1}$$

With ϕ the absorbed photon flux, their recombination (Eq. (2)):

$$e^- + h^+ \xrightarrow{k_R} \Delta \tag{2}$$

And the reaction of photogenerated electrons with water (Eq. (3), mechanistic details in SI):

$$e^- + H_2O \xrightarrow{k_H} \frac{1}{2}H_2 + OH^- \tag{3}$$

From which we can express the H_2 production rate as:

$$Rate_{H_2} = \frac{1}{2}k_H[e^-][H_2O] \tag{4}$$

With k_R the recombination constant and k_H the kinetic constant for water reduction. On the oxidative side, we have to consider the reaction between the photogenerated hole and formic acid with kinetic constant k_f:

$$h^+ + HCOOH \xrightarrow{k_f} HCOO^{\cdot} + H^+ \tag{5}$$

We have to take into account the current doubling of formic acid with kinetic constant k_i: [37]

$$HCOO^{\cdot} \xrightarrow{k_i} e^- + CO_2 + H^+ \tag{6}$$

From this reaction, the CO_2 production rate can be expressed as:

$$Rate_{CO_2} = k_i[HCOO^{\cdot}] \tag{7}$$

Imposing steady state conditions for h^+, e^- and HCOO•, we obtain three algebraic equations:

$$\frac{d[e^-]}{dt} = 0 = \varphi - k_H[e^-][H_2O] - k_R[e^-][h^+] + k_i[HCOO^{\cdot}] \tag{8}$$

$$\frac{d[h^+]}{dt} = 0 = \varphi - k_R[e^-][h^+] - k_f[h^+][HCOOH] \tag{9}$$

$$\frac{d[HCOO^{\cdot}]}{dt} = 0 = k_f[h^+][HCOOH] - k_i[HCOO^{\cdot}] \tag{10}$$

Eq. (10) can be easily solved and the results substituted in Eq. (8), thus obtaining a system of two equations in which k_i does not appear. We solved this reduced system to obtain h^+ and e^-, from which we obtained $Rate_{H2}$ and $Rate_{CO2}$:

$$Rate_{H_2} = Rate_{CO_2} = -a + \sqrt{a(a+2\varphi)} \tag{11}$$

Where:

$$a = \frac{k_H[H_2O]k_f[HCOOH]}{4k_R} \tag{12}$$

In Eq. (11) there is no explicit pH dependence. Therefore, as a first attempt to model the process, we assumed that only the kinetic constant for HCOOH oxidation varies with pH, because of the pH-dependent speciation of formic acid and TiO_2 surface hydroxyls. Within this approximation, the rate constant for HCOOH oxidation k_f must have an electrostatic component. We begin the analysis of this component by considering the electrostatic force F between formic acid and TiO_2, which can be expressed as the summation over n HCOOH molecules and m TiO_2 surface sites:

$$F = k\sum_{i=1}^{n}\sum_{j=1}^{m}\frac{q_i^{HCOOH}q_j^{TiO_2}}{r_{ij}^2} \tag{13}$$

Where k is Coulomb's constant, q_i^{HCOOH} is the charge of the i^{th} formic acid molecule, q_j^{TiO2} is the charge of the j^{th} TiO_2 surface site and r_{ij} is the distance between the i^{th} formic acid molecule and the j^{th} TiO_2 surface site. We remember that the fraction of dissociated HCOOH molecules α_1

is given by Eq. (14):

$$\alpha_1 = \frac{K_a}{[H^+] + K_a} \tag{14}$$

In which K_a is the acid dissociation constant of formic acid. In the summation of Eq. (13) only $\alpha_1$nm terms are non-zero. Substituting r_{ij} with an average distance r and considering that we maintained the same experimental setup and kept the formic acid concentration constant at every pH value, Eq. (13) can be rewritten as:

$$F = -k\frac{[HCOOH]VeN_A\alpha_1}{r^2}\sum_{j=1}^{m} q_j^{TiO_2} = -k'\alpha_1\sum_{j=1}^{m} q_j^{TiO_2} \tag{15}$$

With V the solution volume used in the experiments, N_A the Avogadro's constant, e the elementary charge and with k':

$$k' = k\frac{[HCOOH]VeN_A}{r^2} \tag{16}$$

In Eq. (15) we explicitly introduced a minus sign to account for the negative charge of the conjugate base of formic acid. We can simplify the j index summation analogously: in every experiment we used the same type of TiO_2 (P25) at the same concentration; therefore, we can consider a summation over the p surface site *types* rather than over every m surface site:

$$\sum_{j=1}^{m} q_j^{TiO_2} = ed_{ss}SC_{TiO_2}\sum_{k=1}^{p} q_k\beta_k \tag{17}$$

Where d_{ss} is the surface site density in m^{-2}, S is the specific surface area in $m^2\ g^{-1}$, C_{TiO2} is the TiO_2 concentration used in the photocatalytic experiments, q_k is the charge of the k^{th} surface site type expressed in elementary units and β_k is the fraction of surface sites belonging to the k^{th} type. Substituting Eq. (17) into Eq. (15) we obtain Eq. (18):

$$F = -k'ed_{ss}SC_{TiO_2}V\alpha_1\sum_{k=1}^{p} q_k\beta_k = -k''\alpha_1\sum_{k=1}^{p} q_k\beta_k \tag{18}$$

With all the pH-independent factors contained in k'':

$$k'' = k'ed_{ss}SC_{TiO_2}V \tag{19}$$

Whereas the pH dependence of F can be entirely described by the quantity ζ:

$$\zeta = -\alpha_1\sum_{k=1}^{p} q_k\beta_k \tag{20}$$

Remembering that negative (positive) values represent attractive (repulsive) resultant electrostatic force between substrate and photocatalyst.

To determine ζ as a function of pH, the TiO_2 surface speciation must be known, or, at least, estimated. In their studies Hiemstra et al. [38] demonstrated that in the case of TiO_2, p = 4 and that the four surface site types are linked in two pH-dependent equilibria:

$$\square - TiOH^{-\frac{1}{3}} + H^+ \leftrightarrows \square - TiOH_2^{+\frac{2}{3}} \tag{21}$$

$$\square - Ti_2O^{-\frac{2}{3}} + H^+ \leftrightarrows \square - Ti_2OH^{+\frac{1}{3}} \tag{22}$$

The TiO_2 surface group speciation has been studied by Connor et al. with IR spectroscopy [39], and Bourikas et al. were able to confirm their findings by calculating the TiO_2 surface speciation [40] (reported in Fig. 5) for the {0 0 1} anatase facet using the MUSIC model with a good, even though qualitative, agreement with experimental data. [38] From the β data in Fig. 5, it is possible to calculate ζ as a function of the pH in the case of formic acid (Fig. 6).

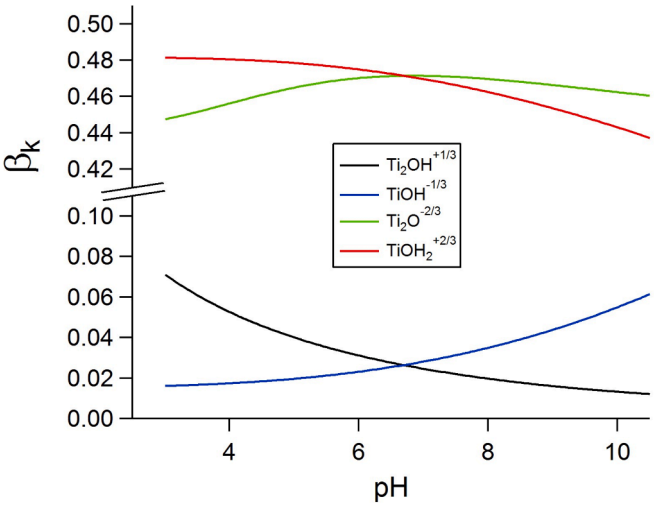

Fig. 5. Calculated speciation of TiO_2 surface calculated for 0.01 M NaCl [38].

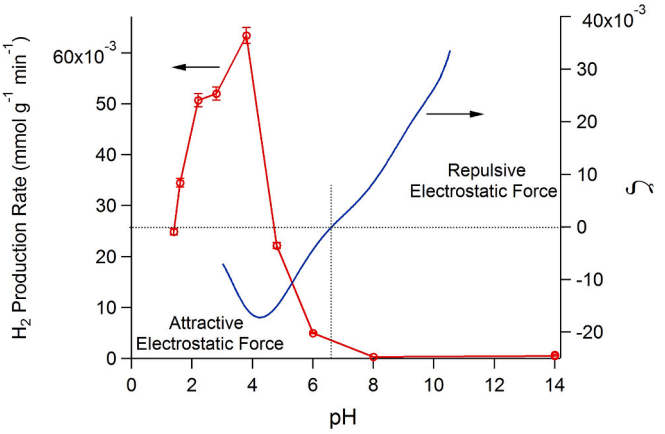

Fig. 6. H_2 production rate for irradiated slurries containing 1 g L^{-1} of P25 TiO_2 and 2 mg L^{-1} of Pt in the presence of HCOOH 0.1 M and the quantity ζ as functions of the pH.

When ζ becomes positive and the electrostatic force is repulsive, the rate is expected to decrease markedly, in good agreement with the observed 100-fold reduction of the rate at basic pH. Nonetheless, the rate remained almost constant at pH 8 and 14, confirming that, concomitant with an inner-sphere direct hole transfer mechanism, an outer-sphere hole transfer or a mediated $HO^{\bullet}$ radical mechanism co-exists. [41,42] The latter are less influenced by electrostatic force, as in the first case solvation can screen electrostatic charges, while in the second a neutral oxidizing species such as $HO^{\bullet}$ is responsible for the oxidation reaction:

$$HO^{\cdot} + HCOOH \overset{k_{HO}}{\rightarrow} HCOO^{\cdot} + H_2O \tag{23}$$

When the electrostatic forces are attractive, the contribution of the outer-sphere or $HO^{\bullet}$ mechanisms to the overall reaction is negligible compared with the direct hole transfer. Conversely, when direct hole transfer is hindered by repulsive electrostatic forces, the other mechanisms prevail and are responsible for the constant trend of the rate at neutral to basic pH values. The kinetic model can be rewritten considering the two contributions, one with an electrostatic-force- and pH-dependent rate constant k_f, and the other with an almost electrostatic-force-independent (and therefore, in our modellistic approach, also pH independent) rate constant k'_f (SI).

We have thus demonstrated that the modelling of the kinetic

constant related to HCOOH oxidation gives satisfactory agreement with the experimental results (Fig. 6). Other possible strategies should involve the other species participating in the overall photocatalytic reaction with pH-dependent speciation: i.e. water and $HCOO^{\bullet}$ radical. In both cases, there would not be agreement with the experiment because $HCOO^{\bullet}$ radical has a pK_a of 1.4, [43] and therefore, it is mostly present in the form $CO_2^{-\bullet}$ in the pH range explored, and could not reproduce the pH dependence of the H_2 production rate.

At this point, it is useful to break down the term a in Eqs. (11) and (12) into two components: $a = -\zeta \cdot J$, in which J contains all the non-electrostatic components of the factor a. The minus sign has been introduced to account for attractive and repulsive electrostatic forces, which have negative and positive signs, respectively. Dividing Eq. (11) by J, we obtain an expression for z, the J-normalized H_2 production rate, which explicitly depends on ζ and therefore on pH:

$$z(\zeta) = \zeta + \sqrt{\zeta\left(\zeta - \frac{2\varphi}{J}\right)} \tag{24}$$

Considering formate radical instead of formic acid, ζ(pH) has a monotonic descending trend, which is reflected in the behaviour of the function z(ζ) (Fig. 7), obtained with $\varphi \bullet J^{-1} = 5$, even though we obtained the same trend with other $\varphi\ J^{-1}$ values (Fig. S2 in SI).

The function z(ζ) gives an estimation of the pH dependence of H_2 production rate within the model presented in the present work. The trend of ζ(pH) (Fig. 7a) reproduces the experiment in the case of the couple $HCOOH/HCOO^-$, but becomes not correlated when formate radical is considered instead. Thus the influence of formate radical, and the rate constant related to its consumption k_i, on the pH dependence of the H_2 evolution rate can be neglected. This result is consistent with the kinetic model (Eqs. (1)–(10)) and the resulting expression of the photocatalytic rate (Eq. (11)), in which the formate radical concentration or the constant k_i do not appear.

In the case of water, the uncharged species H_2O is always at least 1300 times more concentrated than H_3O^+ and 50 times more concentrated than OH– in the pH range explored, and, due to the exponential decrease of H_3O^+ concentration with pH, it is not possible to reproduce the maximum at pH≈4 and the plateau in the basic pH region with arguments as simple and physically sound as we did with the modelling of the formic acid oxidation constant.

A similar behaviour, namely higher rates at acidic pH values, a maximum around pH 5 and a plateau at lower rate values, was observed when CH_3OH was used as the hole scavenger. Even though CH_3OH is a neutral molecule, the considerations made in the case of formic acid can be true here as well, because CH_3OH is converted to CO_2 only after the formation of oxidized intermediates such as HCHO and HCOOH (Fig. 3). [27,29,30] Compared with the case of formic acid, here we not only have to consider coexistence of the inner-sphere direct hole transfer and outer-sphere or HO mediated mechanisms, but also the contribution of HCHO and HCOOH as hole scavengers, generated from the oxidation of CH_3OH. The kinetic analysis is only slightly complicated, as demonstrated in SI, and the system can be reduced to the same form of Equation (11), this time with three kinetic constants k_{f1} k_{f2} k_{f3} related to the oxidation of CH_3OH, HCHO and HCOOH, respectively. Since only HCOOH can be efficiently deprotonated in the pH window explored (2–12), only k_{f3} does depend on pH, whereas k_{f1} and k_{f2}, following our modellistic approach, are pH independent. In this context, we can account for the 20-fold increase of the H_2 production rate observed with CH_3OH at neutral and basic pH (Fig. 2) compared with formic acid (Fig. 1). Beyond pH 6, k_{f3} is expected to decrease significantly, and, in the presence of formic acid alone, recombination with photoelectrons becomes the most probable reaction path for photogenerated holes with the consequent depression of H_2 evolution. With CH_3OH, the photogenerated holes can react with CH_3OH and HCHO with rate constant k_{f1} and k_{f2}, respectively; recombination is then limited, and H_2 production is 20 times higher.

Since the same behaviour of H_2 production rate as a function of pH is observed when Pt is deposited in a former photochemical step (pH3-Pt-P25, Fig. 4), we can exclude that the observed trend is due to a different efficiency in the Pt deposition step, even if performed starting from a negatively charged complex, [35] and further validate the models proposed for the understanding of the photocatalytic process and estimation of the rate constant related to formic acid oxidation.

The results obtained with the model proposed could be qualitatively, but not completely correctly, summarized in terms of formic acid speciation and TiO_2 surface charging: in synthesis at pH values lower than the point of zero charge PZC of TiO_2, the rate is higher, while for pH > PZC the reaction becomes slower, and the experimental trend could also be interpreted in terms of formic acid adsorption. This kind of statement should be considered carefully because, even if it appears true for formic acid, a C1 species giving current doubling and therefore with very limited back reactions, it could be misleading with other substrates if back reactions are important. [36] This is the reason why we had to model the photocatalytic reactions *before*, obtaining analytical

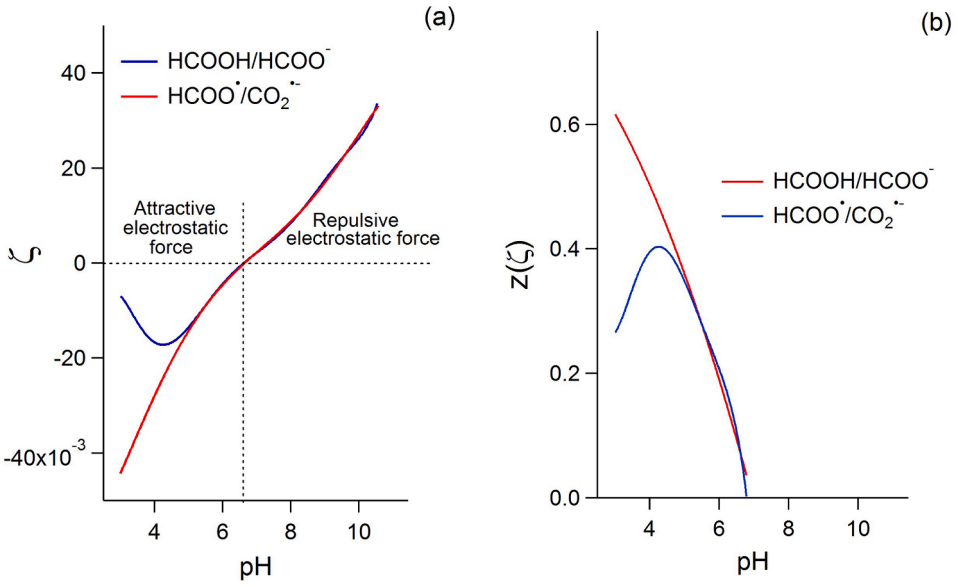

Fig. 7. ζ (panel a) and z(ζ) (panel b) as functions of the pH for the couples $HCOOH/HCOO^-$ ($pK_a = 3.8$) and $HCOO^{\bullet}/CO_2^{-\bullet}$ ($pK_a = 1.4$).

expressions for the rates, and only in a second stage did we try to reproduce the experimental pH dependence. This approach could be extremely useful in the study of biomass photoreforming, where different families of compounds can be present simultaneously, [33,44,45] and certain among them can react with both photogenerated electrons and holes, [46] resulting in peculiar, – and often hard to rationalize – pH dependence of the H_2 production rate and, to complicate the matter, sometimes conflicting evidences were reported. [32–34].

5. Conclusion

We observed that the photocatalytic reforming of formic acid and methanol displays similar pH dependence. In both cases we noticed high rates at acidic pH values, with a maximum around pH 4–5 and a lower plateau at neutral and basic pH values. The kinetic model of the overall reaction allowed us to write an expression for H_2 and CO_2 production rate, but without explicit pH dependence. We therefore assumed that pH dependence could be hidden in the rate constant related to the reaction between formic acid and photogenerated holes, in the form of the resultant electrostatic force between formic acid and the TiO_2 surface. With this approach, we found good agreement with the experiment and confirmed the coexistence of a direct hole transfer and an HO radical-mediated mechanism. We also highlighted the importance of the speciation of the substrate and TiO_2 surface groups, which play a crucial role in the modulation of their interaction, and therefore in the determination of the overall reaction rate. These considerations were successfully extended to the photocatalytic reforming of other carboxylic acids and methanol, which produce formic acid by oxidation during irradiation, providing additional support for the combined approach adopted.

CRediT authorship contribution statement

Fabrizio Sordello: Writing – review & editing, Writing – original draft, Methodology, Investigation, Formal analysis, Conceptualization.

Declaration of competing interest

The authors declare that they have no known competing financial interests or personal relationships that could have appeared to influence the work reported in this paper.

Acknowledgements

Financial support from Università degli Studi di Torino (Ricerca Locale) is gratefully acknowledged.

FS thanks Mr. Jack Jia Xin Song for proofreading the article.

Appendix A. Supplementary data

Supplementary data to this article can be found online at https://doi.org/10.1016/j.jphotochem.2024.116205.

Data availability

Data will be made available on request.

References

[1] V. Smil, Energy Transitions: Global and National Perspectives, 2nd ed., ABC-CLIO, Santa Barbara, California (USA), 2017.
[2] N. Armaroli, V. Balzani, The future of energy supply: challenges and opportunities, Angew. Chem.-Int. Edit. 46 (2007) 52–66.
[3] S.Y. Reece, J.A. Hamel, K. Sung, T.D. Jarvi, A.J. Esswein, J.J.H. Pijpers, D. G. Nocera, Wireless solar water splitting using silicon-based semiconductors and earth-abundant catalysts, Science 334 (2011) 645–648.
[4] F.E. Osterloh, Inorganic nanostructures for photoelectrochemical and photocatalytic water splitting, Chem. Soc. Rev. 42 (2013) 2294–2320.
[5] H. Tributsch, B. Neumann, Material research challenges towards a corrosion stable photovoltaic hydrogen-generating membrane, Int. J. Hydrogen Energy 32 (2007) 2679–2688.
[6] H. Tributsch, Photovoltaic hydrogen generation, Int. J. Hydrogen Energy 33 (2008) 5911–5930.
[7] H. Pan, Principles on design and fabrication of nanomaterials as photocatalysts for water-splitting, Renew. Sustain. Energy Rev. 57 (2016) 584–601.
[8] F. Sordello, P. Calza, C. Minero, S. Malato, M. Minella, More than one century of history for photocatalysis, from past, present and future perspectives, Catalysts (2022).
[9] G. Peharz, F. Dimroth, U. Wittstadt, Solar hydrogen production by water splitting with a conversion efficiency of 18%, Int. J. Hydrogen Energy 32 (2007) 3248–3252.
[10] H. Nishiyama, T. Yamada, M. Nakabayashi, Y. Maehara, M. Yamaguchi, Y. Kuromiya, H. Tokudome, S. Akiyama, T. Watanabe, R. Narushima, S. Okunaka, N. Shibata, T. Takata, T. Hisatomi, K. Domen, Photocatalytic solar hydrogen production from water on a 100 m2-scale, Nature (2021).
[11] Z. Li, W. Luo, M. Zhang, J. Feng, Z. Zou, Photoelectrochemical cells for solar hydrogen production: current state of promising photoelectrodes, methods to improve their properties, and outlook, Energy Environ. Sci. 6 (2013) 347–370.
[12] K. Lee, R. Hahn, M. Altomare, E. Selli, P. Schmuki, Intrinsic Au decoration of growing TiO2 nanotubes and formation of a high-efficiency photocatalyst for H2 production, Adv. Mater. 25 (2013) 6133–6137.
[13] G.L. Chiarello, M.V. Dozzi, M. Scavini, J.D. Grunwaldt, E. Selli, One step flame-made fluorinated Pt/TiO2 photocatalysts for hydrogen production, Appl. Catal. B: Environ. 160–161 (2014) 144–151.
[14] Q. Wang, K. Domen, Particulate photocatalysts for light-driven water splitting: mechanisms, challenges, and design strategies, Chem. Rev. 120 (2020) 919–985.
[15] J. Fu, K. Jiang, X. Qiu, J. Yu, M. Liu, Product selectivity of photocatalytic CO2 reduction reactions, Mater. Today 32 (2020) 222–243.
[16] C. Zhang, H. Wang, H. Yu, K. Yi, W. Zhang, X. Yuan, J. Huang, Y. Deng, G. Zeng, Single-atom catalysts for hydrogen generation: rational design, recent advances, and perspectives, Adv. Energy Mater. 12 (2022).
[17] S. Singla, S. Sharma, S. Basu, N.P. Shetti, T.M. Aminabhavi, Photocatalytic water splitting hydrogen production via environmental benign carbon based nanomaterials, Int. J. Hydrogen Energy 46 (2021) 33696–33717.
[18] M. Tahir, S. Tasleem, B. Tahir, Recent development in band engineering of binary semiconductor materials for solar driven photocatalytic hydrogen production, Int. J. Hydrogen Energy 45 (2020) 15985–16038.
[19] M. Ismael, A review and recent advances in solar-to-hydrogen energy conversion based on photocatalytic water splitting over doped-TiO2 nanoparticles, Sol. Energy 211 (2020) 522–546.
[20] H.J. Yun, H. Lee, J.B. Joo, N.D. Kim, J. Yi, Effect of TiO2 nanoparticle shape on hydrogen evolution via water splitting, J. Nanosci. Nanotechnol. 11 (2011) 1688–1691.
[21] F. Pellegrino, F. Sordello, L. Mino, C. Minero, V.-D. Hodoroaba, G. Martra, V. Maurino, Formic acid photoreforming for hydrogen production on shape-controlled anatase TiO2 nanoparticles: assessment of the role of fluorides, {101}/{001} surfaces ratio, and platinization, ACS Catal. 9 (2019) 6692–6697.
[22] F. Sordello, C. Minero, Photocatalytic hydrogen production on Pt-loaded TiO2 inverse opals, Appl. Catal. B: Environ. 163 (2015) 452–458.
[23] M.V. Dozzi, G.L. Chiarello, M. Pedroni, S. Livraghi, E. Giamello, E. Selli, High photocatalytic hydrogen production on Cu(II) pre-grafted Pt/TiO2, Appl. Catal. B: Environ. 209 (2017) 417–428.
[24] F. Sordello, M. Prozzi, V.-D. Hodoroaba, J. Radnik, F. Pellegrino, Increasing the HER efficiency of photodeposited metal nanoparticles over TiO2 using controlled periodic illumination, J. Catal. 429 (2024) 115215.
[25] A. Naldoni, M. D'Arienzo, M. Altomare, M. Marelli, R. Scotti, F. Morazzoni, E. Selli, V. Dal Santo, Pt and Au/TiO2 photocatalysts for methanol reforming: role of metal nanoparticles in tuning charge trapping properties and photoefficiency, Appl. Catal. B: Environ. 130–131 (2013) 239–248.
[26] Y.-H. Fang, G.-F. Wei, Z.-P. Liu, Catalytic role of minority species and minority sites for electrochemical hydrogen evolution on metals: surface charging, coverage, and tafel kinetics, J. Phys. Chem. C 117 (2013) 7669–7680.
[27] T. Chen, Z. Feng, G. Wu, J. Shi, G. Ma, P. Ying, C. Li, Mechanistic studies of photocatalytic reaction of methanol for hydrogen production on Pt/TiO2 by in situ Fourier transform IR and time-resolved IR spectroscopy, J. Phys. Chem. C 111 (2007) 8005–8014.
[28] J. Kennedy, H. Bahruji, M. Bowker, P.R. Davies, E. Bouleghlimat, S. Issarapanacheewin, Hydrogen generation by photocatalytic reforming of potential biofuels: polyols, cyclic alcohols, and saccharides, J. Photochem. Photobiol. A Chem. 356 (2018) 451–456.
[29] H. Bahruji, M. Bowker, P.R. Davies, F. Pedrono, New insights into the mechanism of photocatalytic reforming on Pd/TiO2, Appl. Catal. B: Environ. 107 (2011) 205–209.
[30] G.L. Chiarello, M.H. Aguirre, E. Selli, Hydrogen production by photocatalytic steam reforming of methanol on noble metal-modified TiO2, J. Catal. 273 (2010) 182–190.
[31] L.-F. Wei, X.-J. Zheng, Z.-H. Zhang, Y.-J. Wei, B. Xie, M.-B. Wei, X.-L. Sun, A systematic study of photocatalytic H2 production from propionic acid solution over Pt/TiO2 photocatalyst, Int. J. Energy Res. 36 (2012) 75–86.
[32] X. Fu, J. Long, X. Wang, D.Y.C. Leung, Z. Ding, L. Wu, Z. Zhang, Z. Li, X. Fu, Photocatalytic reforming of biomass: a systematic study of hydrogen evolution from glucose solution, Int. J. Hydrogen Energy 33 (2008) 6484–6491.

[33] F. Conte, G. Casalini, L. Prati, G. Ramis, I. Rossetti, Photoreforming of model carbohydrate mixtures from pulping industry wastewaters, Int. J. Hydrogen Energy 47 (2022) 41236–41248.
[34] G. Iervolino, V. Vaiano, J.J. Murcia, L. Rizzo, G. Ventre, G. Pepe, P. Campiglia, M. C. Hidalgo, J.A. Navío, D. Sannino, Photocatalytic hydrogen production from degradation of glucose over fluorinated and platinized TiO2 catalysts, J. Catal. 339 (2016) 47–56.
[35] J. Kiwi, M. Graetzel, Optimization of conditions for photochemical water cleavage. Aqueous platinum/TiO2 (anatase) dispersions under ultraviolet light, J. Phys. Chem. 88 (1984) 1302–1307.
[36] C. Minero, D. Vione, A quantitative evaluation of the photocatalytic performance of TiO2 slurries, Appl. Catal. B: Environ. 67 (2006) 257–269.
[37] T.L. Villarreal, R. Gómez, M. González, P. Salvador, A kinetic model for distinguishing between direct and indirect interfacial hole transfer in the heterogeneous photooxidation of dissolved organics on TiO2 nanoparticle suspensions, J. Phys. Chem. B 108 (2004) 20278–20290.
[38] T. Hiemstra, P. Venema, W.H.V. Riemsdijk, Intrinsic proton affinity of reactive surface groups of metal (hydr)oxides: the bond valence principle, J. Colloid Interface Sci. 184 (1996) 680–692.
[39] P.A. Connor, K.D. Dobson, A.J. McQuillan, Infrared spectroscopy of the TiO2/aqueous solution interface, Langmuir 15 (1999) 2402–2408.
[40] K. Bourikas, T. Hiemstra, W.H. Van Riemsdijk, Ion pair formation and primary charging behavior of titanium oxide (anatase and rutile), Langmuir 17 (2001) 749–756.
[41] Y. Sun, J.J. Pignatello, Evidence for a surface dual hole-radical mechanism in the titanium dioxide photocatalytic oxidation of 2,4-D, Environ. Sci. Technol. 29 (1995) 2065–2072.
[42] P. Calza, M. Minella, L. Demarchis, F. Sordello, C. Minero, Photocatalytic rate dependence on light absorption properties of different TiO2 specimens, Catal. Today 340 (2020) 12–18.
[43] G.V. Buxton, R.M. Sellers, Acid dissociation constant of the carboxyl radical. Pulse radiolysis studies of aqueous solutions of formic acid and sodium formate, J. Chem. Soc., Faraday Trans. 1 69 (1973).
[44] L. Lan, H. Daly, R. Sung, F. Tuna, N. Skillen, P.K.J. Robertson, C. Hardacre, X. Fan, Mechanistic study of glucose photoreforming over TiO2-based catalysts for H2 production, ACS Catal. 13 (2023) 8574–8587.
[45] M. Aljohani, H. Daly, L. Lan, A. Mavridis, M. Lindley, S.J. Haigh, C. D'Agostino, X. Fan, C. Hardacre, Enhancing Hydrogen Production from the Photoreforming of Lignin, ChemPlusChem 89 (2024) e202300411.
[46] K.E. Sanwald, T.F. Berto, W. Eisenreich, A. Jentys, O.Y. Gutiérrez, J.A. Lercher, Overcoming the rate-limiting reaction during photoreforming of sugar aldoses for H2-generation, ACS Catal. 7 (2017) 3236–3244.